ICCBT2008

Water-powder Mixtures at the Onset of Flowing

M. Hunger*, University of Twente, ***THE NETHERLANDS***
H. J. H. Brouwers, University of Twente**, *THE NETHERLANDS***

ABSTRACT

The knowledge of water demands of the manifold concrete ingredients is of vital interest for the design of concrete mixes. Physical properties like workability or strength and durability in hardened state are controlled by the total water content. Water demand is defined as the volumetric ratio of water to solid material at a certain state, which is defined by the selected test method. Given that powders provide the b far highest percentage of specific surface area in a concrete mixture, their water demand is of special interest. In literature diverse methods for the determination of powders' water demands can be found. However, it appears that the spread-flow test, sometimes referred to as mini-slump flow test, has achieved general acceptance in concrete technology. In this research the spread-flow test has been analyzed in more detail. In this way new measures are derived which contribute to a deeper understanding of wet granular mixtures at the onset of flowing. The deformation coefficient which will be derived by the spread-flow test was confirmed to correlate with the product of Blaine surface and intrinsic density of the individual powders when the mixture is flowing only under its own weight. Similarly, correlations with equal accuracy have been found with a computed specific surface based on measured particle size distributions instead of the Blaine surface. Using flow experiments it was possible to derive an overall factor for assessing the non-spherical shape of the powder particles. A good correlation of this computation algorithm was derived compared to the standard Blaine method. Finally, a constant water layer thickness around the powder particles was derived for all powders at the onset of flowing. This implies the possibility to predict flow behavior of mortar and concrete mixtures only based on the knowledge of their granular characteristics.

Keywords: *Water demand, Spread-flow test, Constant Water layers, Specific surface area, Blaine.*

**Correspondence Author: Martin Hunger, University of Twente, The Netherlands. Tel: +31 (0)53 489 6863, Fax: +31 (0)53 489 2511. E-mail: m.hunger@ctw.utwente.nl*

1. INTRODUCTION

The water demand of powders, the finest particles in concrete, is a significant parameter for the design of concrete. It is composed of a layer of adsorbed water molecules around the particles and an additional amount needed to fill the intergranular voids of the powder system. Since powders provide by far the biggest part of the total specific surface area, they have the strongest influence on the total water demand of a concrete mix. Consequently, they should have a preferably low water demand. The spread-flow test is, amongst others, a suitable test procedure for the determination of water demands of powders, mortars and even complete concrete mixtures.

Literature [1] shows that the execution of spread-flow tests is not only limited to water/powder ratios indicating the onset of flowing. Rather, this test seems to provide more information on the relation of water demand sufficient for flowing, void fraction, and the influence of specific surface area on the variation of fluidity. In this regard, [1] found a linear relation between specific surface area and the relative slump when sufficient water is present for flow. This hypothesis is going to be addressed in the following.

2. FLOW EXPERIMENTS

The spread-flow test (or sometimes referred to as paste line test or mini-slump flow test) according to [2] appears to be the classical method for the determination of the water demand of powder materials involved in SCC. Thereby suspensions are produced being composed of the powder to be analyzed and varying quantities of water. After appropriate mixing following a defined mix regime, the suspension is filled in a special conical mold in the form of a frustrum, the Hägermann cone, which is lifted straight upwards in order to allow free flow for the paste without any jolting. In contrast to several literary sources [3] the obtained paste is not filled in two layers with intermediate compaction but in one into the cone, as its flow behavior solely due to own weight is going to be analyzed. This therefore also holds for the compaction. The recommended working surface for this test is a dry, clean, horizontal and non sucking surface (best is a glass plate). From the spread-flow of the paste, two diameters perpendicular to each other (d_1 and d_2) can be determined. Their mean is deployed to compute the relative slump (Γ_p) via:

$$\Gamma_p = \left(\frac{d}{d_0}\right)^2 - 1 \qquad with\ d = \frac{d_1 + d_2}{2} \tag{1}$$

where d_0 represents the base diameter of the used cone, 100 mm in case of the Hägermann cone. The relative slump Γ_p is a measure for the deformability of the mixture, which was originally introduced by [2] as relative flow area R.

At least four different water/powder-ratios have to be tested to obtain a statistically reliable trend line. Thereby, new water/powder-ratios are realized by preparing new mixes and explicitly not by adding water to the present mix. It is furthermore recommended [4] to aim on spread-flows of 140 mm up to 230 mm, which corresponds to a relative slump Γ_p of 0.96 to 4.29 using the Hägermann cone. Other literature [3] refers to a range from 0.2 to 15. It is believed that any spread-flow can be accepted for assessment, as long as it shows a measurable

and symmetrical spread, and possesses no signs of segregation (obvious centric pile) or bleeding (corona of bleeding water).

By means of a graphical analysis (cp.Figure 1) all measured Γ_p are plotted versus their respective water/powder volume ratios (V_w/V_p) involving the respective specific densities of the deployed materials. A straight line is fitted through the derived data points afterwards. The intersection of this linear function with the axis of ordinates at $\Gamma_p = 0$ depicts the retained water ratio where no slump takes place [5]. In other words, this denotes the maximum amount of water which can be retained by the particles. Exceeding this water content will turn the coherent bulk into a concentrated suspension. This point is referred to as water demand or retained water ratio, which was introduced as β_p in the field of concrete.

From the measurement, a linear relation can be computed for each material with the help of linear regression. The outcome of this analysis is a function of the type:

$$\frac{V_w}{V_p} = E_p \, \Gamma_p + \beta_p \tag{2}$$

Besides the water demand β_p, information is also provided by the value E_p, the deformation coefficient, which is the slope of the function. This value can be understood as a measure of sensitivity on the water need for a specified flowability. That means materials showing a lower E_p, hence having flat slopes, respond with bigger change in deformability to a certain change in water dosage than materials having a steeper slope. Thus small changes in the water content have a stronger influence on the relative slump. In this way, materials can be identified that tend sooner to bleeding or segregation than other materials in mortars and concrete mixes. The probability of this negative behavior becomes higher with decreasing amount of cement and with high amounts of powder materials exhibiting strong sensitivity to water changes (low E_p-values).

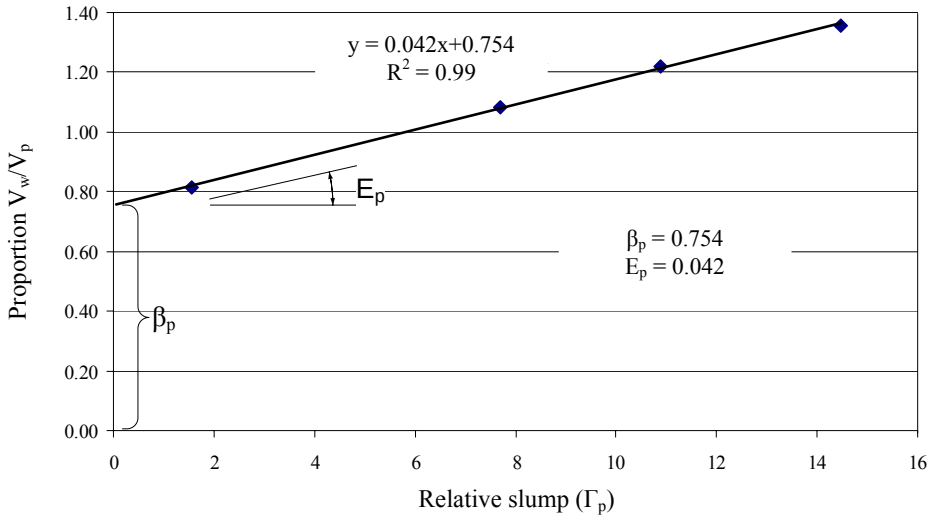

Figure 1. Principle of a spread-flow experiment, showing varying water/powder proportions as a function of the relative slump flow.

3. ANALYSIS OF FLOW EXPERIMENTS

3.1 Derivation of a shape factor based on flow experiments

In the following the derivation of a shape factor, based on flow experiments with water-powder mixtures, is described. This procedure will indirectly provide a shape factor, not being based on direct measurements of particle dimensions, but relevant for water–powder flow. The particle shape factor is expressing the ratio of an effective particle surface area of an irregularly formed particle to the surface area of an ideal sphere with equal volume. According to this definition, the ideal, smooth sphere would have a shape factor, ξ, of 1. This represents a three-dimensional approach, being based on volume considerations. In principle two approaches are reported in literature. On the one hand two-dimensional particle shape measurements are conducted with the help of images or projections. On the other hand three-dimensional analysis with individual particles is possible by measuring the principal axes of an irregularly shaped particle. Both approaches are direct measurements as specific geometrical characteristics of a particle are considered.

Besides the classical approach of directly measuring particle dimensions there are also indirect ways to derive an overall shape factor. The above described methods provide a number of measures, which can describe particles in detail. However, their combination to an overall-shape factor turned out to be difficult. Motivated by the varied usage of shape factors, there is an interest to find suitable values with more general measurement techniques or in other words to find correlations with values measured anyway. One approach was for example given in [6], who is forming a ratio of the directly measured Blaine surface a_{Blaine} and the computed surface area a via:

$$\xi_{\mathrm{Re}\,schke} = \frac{a_{Blaine}}{a} \tag{3}$$

The computed surface area, *a,* was thereby developed from the particle size distribution, assuming spheres with equivalent diameter. So, [6] used Blaine values to calibrate and derive shape factors. Therefore, the obtained shape factors still contain the systematical error involved with the Blaine measurement. Subsequent to the computation of the shape factors their plausibility was verified by SEM-documentation of selected powder materials. Analyzing the results obtained, groups of similar materials were formed when organizing the shape factors in ascending order, i.e. generalized each material type is forming narrow ranges of shape factors.

In total Reschke determines a range of shape factors $\xi_{Reschke}$ from 1.00 up to 3.08, of which 1.00 represents micro-glass spheres and 3.08 a kaolin type. However, the value for the micro-glass spheres was not measured but assumed to be unity. Therefore this model cannot be considered to be aligned with the ideal model case. Summarizing, this model gives plausible results being in line with the SEM-image analysis.

In order to compute specific surface data, the particle shape data provided in [6] was, for the time being, used to correct the computed surface area for the non-spherical particle shape. In the following, a model for the computation of shape factors will be derived based on flow experiments. Then, these values based on Reschke are used for comparative purposes. In Table

1 the selected shape factors are given in combination with the sphere-based surface area, as well as with the shape corrected surface area.

Table 1. Surface area properties of the powders

Material	Specific surface area				
	Blaine a_{Blaine} [cm^2/g]	BET a_{BET} [m^2/kg]	Computed sphere based S_{sph} [cm^2/cm^3]	Shape factor $\xi_{Reschke}$	Computed Non-spherical S [cm^2/cm^3]
CEM I 52.5 R - micro cement	-	2,200	26,624	1.68	44,728
CEM I 52.5 N	-	-	15,749	1.68	26,458
CEM III/B 42.5 N A	4,830	-	12,687	1.58	20,045
CEM III/B 42.5 N B	4,500	-	17,775	1.58	28,085
Limestone powder	4,040	-	13,850	1.26	17,451
Granite powder	-	-	13,051	1.50	19,577
Marble powder A	4,580	-	14,739	1.50	22,109
Marble powder B	-	-	12,573	1.50	18,860
Marble powder C	-	-	13,391	1.50	20,087
Fly ash A	2,840	-	13,113	1.20	15,736
Fly ash B	-	-	13,419	1.20	16,103
Gypsum A	-	-	7,970	1.80	14,346
Gypsum B	-	-	9,713	1.80	17,483
Trass	-	-	15,603	1.20	18,724

One of the major hypothesis put forward by [1] was that the relative slump of a water-powder mixture becomes a function of the specific surface area when sufficient water is present for flow, i.e. $V_w/V_p > \beta_p$. This hypothesis was validated by relating the slope of the spread-flow function E_p (cp. Eq. (2)), the deformation coefficient, to the specific surface area S. The specific surface area was taken from Blaine (a_{Blaine}) multiplied by the specific particle density ρ_s to obtain the specific area per volume of powder. From the observations it was concluded that the larger the internal surface, the larger the deformation coefficient (the more water is required to attain a certain relative slump). Accordingly, the following linear relation was derived:

$$E_p = \delta \cdot a_{Blaine} \cdot \rho_s = \delta \cdot S \tag{4}$$

with δ representing the thickness of an idealized water layer, surrounding the particles of a water-powder dispersion with $V_w/V_p = \beta_p$, i.e. the onset of flowing. [1] found a mean δ of 41.32 nm, which is incidentally in the same magnitude as the interfacial transition zone (ITZ) in concrete. This range was also confirmed by [7], who found a layer thickness of about 150 water molecules for the water demand of particle fractions by means of sorption experiments. This layer thickness corresponds to approximately 45 nm as the size of one water molecule is about 3 Å.

In this section the above approach is applied for the derivation of a shape factor, considering a larger number of powder samples. A further modification is introduced by the substitution of the Blaine surface area by the uncorrected, computed specific surface area a_{sph}. This PSD-based computed surface area is a weight-based measure like the Blaine surface too and is chosen since the Blaine measurement holds some uncertainty in itself, especially for powders of

high fineness, since the Carman-Kozeny equation used in air permeability method is not valid for particles smaller than 10 μm [8]. In principle the computational models for laser diffraction and the measurement itself also contain some inaccuracy, but no systematical error is additionally introduced, as it would be the case by using Blaine measurements. Since the derived shape factor will later be applied on the detailed PSD, containing the same systematical error, there will be no multiplied effect on the corrected computed surface area. Furthermore, the PSD data is available and Blaine does not need to be determined in addition. Blaine-test and computed surface area both describe the outer surface of particles and apart from a systematic deviation due to different measurement principles they provide basically the same information. This is also confirmed in [9].

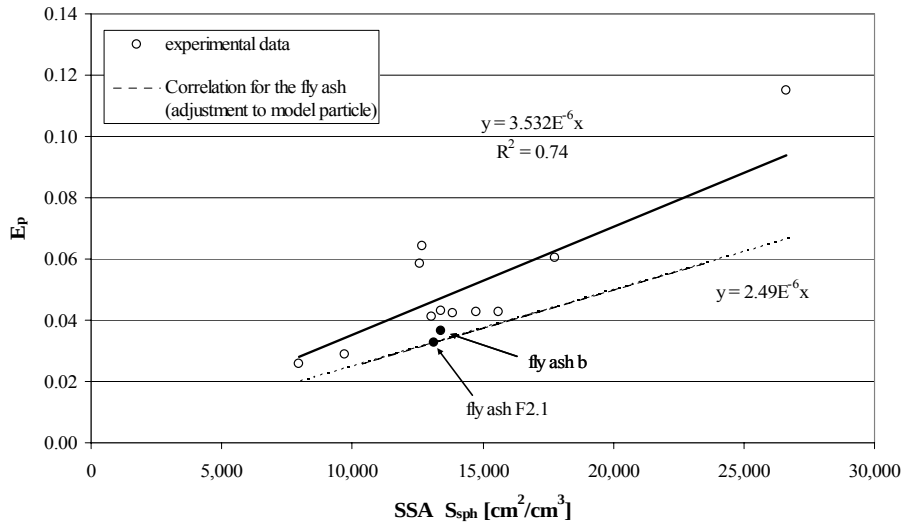

Figure 2. Plot of uncorrected, computed and volume based specific surface areas against the respective deformation coefficient E_p derived from spread-flow tests.

Now, plotting the computed specific surface area (S_{sph}) of these powders against the deformation coefficient E_p, Figure 2 is obtained. Figure 2 provides the necessary results of the spread-flow tests on these powder materials. Note that E_p, β_p and S_{sph} used in this graph are all volume based, and S_{sph} is the specific surface if the particles would be truly spherical. With the help of linear regression a relation was derived for these measures. Based on the assumption that the slope of a paste line becomes a function of SSA when $V_w/V_p > \beta_p$ is satisfied, the regression line has to intercept the point $E_p = 0$. Now, assuming straight lines from every data point through the origin would result in lowest slopes for the two fly ash powders involved, the two materials with the most spherical shape. Their true surface will namely be closest to the actual one, as they are close to spherical shape. As the computation of SSA is based on the assumption of spheres, a shape factor larger than unity (i.e. $\xi > 1$) is necessary to correct for non-spherical shape, i.e. a positive displacement of all data points parallel to the axis of abscissa (increase of SSA). Hence, the material having the lowest slope (δ) could serve as model particle to calibrate the others. Finding the lowest slope for the materials with the most sphere-like shape could already serve as a simple validation of the presented approach.

In order to further validate the proposed relation between S_{sph} and E_p, shape factors have been selected in a next step. This selection was based on the work in [6] and is not related to measured properties of the materials evaluated. In this way the different cement types were as-

signed with same shape factors of equivalent cement types from Reschke's research, e.g. a limestone powder was given the averaged shape factor for limestone powders taken from Reschke. These selected shape factors are given in Table 1. It should be understood that they will only serve as a first comparison. Plotting these newly derived and now shape-corrected SSAs against E_p results in an improved coefficient of determination.

Table 2. Surface area properties of the powders

Material	Deformation coefficient E_p [-]	Parameter for water layer thickness δ [cm]	Water demand β_p [-]
Granite powder	0.0410	3.14×10^{-6}	1.2151
CEM III/B 42.5 N A	0.0643	5.07×10^{-6}	0.976
CEM III/B 42.5 N B	0.0603	3.39×10^{-6}	1.124
CEM I 52.5 R - micro cement	0.1151	4.32×10^{-6}	1.730
Fly ash A*	0.0327	2.49×10^{-6}	0.524
Fly ash B	0.0366	2.73×10^{-6}	0.532
Limestone powder	0.0422	3.05×10^{-6}	0.754
Marble powder A	0.0426	2.89×10^{-6}	0.874
Marble powder B	0.0585	4.65×10^{-6}	1.005
Marble powder C	0.0432	3.23×10^{-6}	0.829
Gypsum A	0.0259	3.25×10^{-6}	0.673
Gypsum B	0.0287	2.95×10^{-6}	0.579
Trass	0.0428	2.74×10^{-6}	1.061

* The fly ash is used as calibration standard for the shape factor computation

Based on these considerations a particle shape factor ξ was derived to correct all available and only sphere-based SSA in such a way that they fit on the regression line given by the particles that come closest to spherical shape (i.e. $\xi = 1$), which in this case is fly ash (cp. Figure 2). The equation based on the fly ash then reads as:

$$E_p = \delta \cdot a \cdot \rho_s = 2.49 \cdot 10^{-6}\, cm \cdot S\,, \qquad with\ \delta = 2.49 \cdot 10^{-6}\, cm \tag{5}$$

Now, substituting E_p with the associated deformation coefficients determined by the spread-flow experiments and assuming a film thickness of 24.9 nm, for every material, a theoretical specific surface area S is computed. Comparing this theoretical surface with the uncorrected surface S_{sph}, with ξ set equal to unity, a new shape correction factor ξ can be derived. This factor reads as:

$$\xi = \frac{S}{S_{sph}} \tag{6}$$

Applying Eq. (6), shape factors have been computed for all given materials. These factors can be found in Table 3. The corresponding shape factors, chosen on the basis of [6] are included in the same table as well. Comparing the data obtained, it can be noticed that derived shape factors correlate well with the ones based on Reschke. This further validates the approach followed here. In total the shape factors range from 1.00 for the fly ash (as imposed here) up to

2.03 for the CEM III/B 42.5 N, the latter appearing to have the biggest shape deviation from smooth spheres. Note that all shape factors are larger than unity indeed, which is consistent with the proposed approach. The second type of fly ash (fly ash B) yields a shape factor only slightly higher than fly ash A. Differences in fly ash shape factors, also notably higher ones, can be explained by the partly porous surface structure, fly ash can possess. The surface structure of fly ash is highly dependent on the formation conditions. Furthermore, fly ash also can contain other types of ashes, unburnt coke particles, quartz particles or broken hollow balls. However, the assumed spherical shape, $\xi_{FA} = 1$, seems to be a good basis. Furthermore, if fly ash would turn out to have a shape factor slightly larger than unity, all shape factors derived here only need to be multiplied with this $\xi_{FA} > 1$.

Table 3. Shape factors, ξ, based on Reschke [6] and on the presented study

Material	Shape factor based on Reschke [6] $\xi_{Reschke}$	Shape factor Computed by present study ξ
Granite powder	1.50	1.26
CEM III/B 42.5 N A	1.58	2.03
CEM III/B 42.5 N B	1.58	1.36
CEM I 52.5 R - micro cement	1.68	1.73
Fly ash A	1.20	1.00
Fly ash B	1.20	1.09
Limestone powder	1.26	1.22
Marble powder A	1.50	1.16
Marble powder B	1.50	1.87
Marble powder C	1.50	1.29
Gypsum A	1.80	1.30
Gypsum B	1.80	1.18
Trass flour	1.20	1.10

3.2 SEM image analysis

In order to further validate the derived shape factors and in particular to distinguish between particle geometry and surface roughness, SEM micrographs have been prepared and analyzed. The SEM images with a magnification factor of 1,000 are exemplarily given in Figure 3 (a-f). Thereby the order of appearance from (a) to (f) corresponds to increasing shape factors as determined here (Table 3). The glass beads (a) have not been introduced to the measurement yet since their monosized-like behavior causes problems during the spread-flow tests. However, their ideal spherical shape and the smooth surface justifies an application as model particles for adjusting the shape factor derivation. Next, the fly ash A (b) is for the most part composed of spherical particles but like described earlier to some extent they show porous surfaces or contain other materials. The dolomitic marble powder A (c) is already notable less spherical but still providing a smooth surface, which explains the only slightly higher shape factor. A similar situation can be observed for the limestone powder (d) but here the surface appears to be rougher, resulting in a higher shape factor. The blast-furnace cement (e) shows highly angular shapes for the ground slag particles but having a smooth surface. Therefore, the shape factor still is comparable with for example the limestone powder. Finally, the micro cement (f) shows angular particles with rough surface and therefore achieves the highest shape factor

for this set of selected powders. This visual analysis strengthens the computational model and the shape factors derived here.

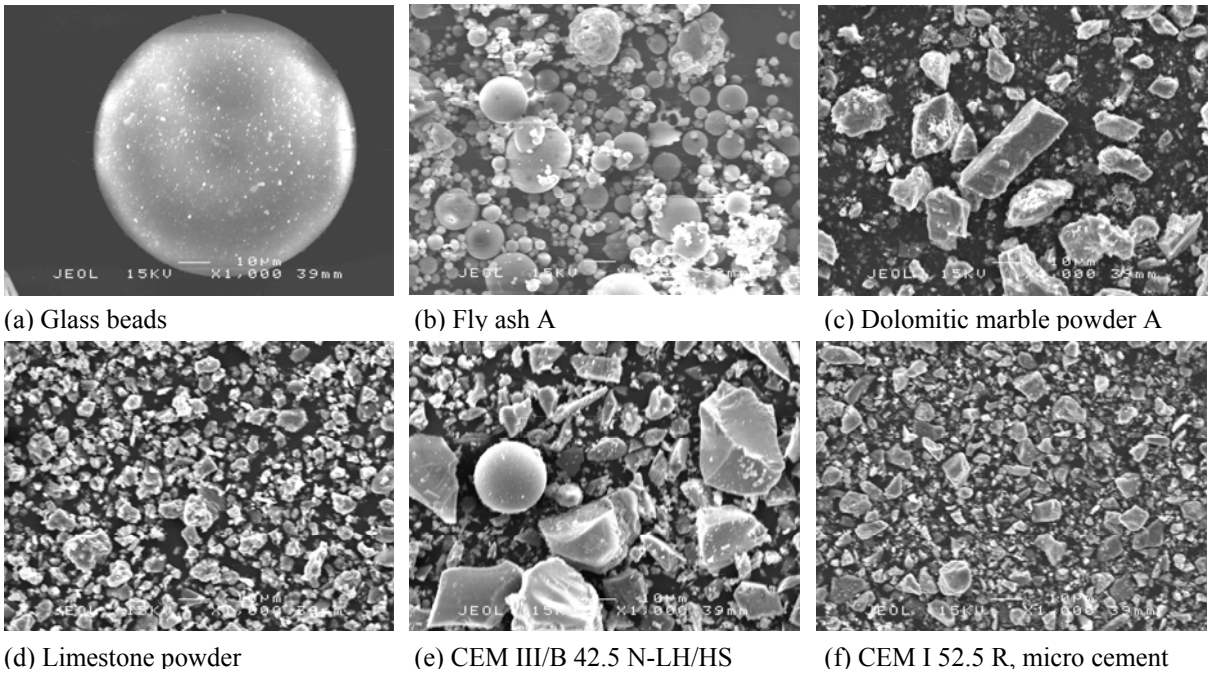

(a) Glass beads (b) Fly ash A (c) Dolomitic marble powder A

(d) Limestone powder (e) CEM III/B 42.5 N-LH/HS (f) CEM I 52.5 R, micro cement

Figure 3. SEM micrographs of the investigated powders, 1,000-times magnified.

3.3 Concept of constant water layer thickness

From Eq. (3) a value of 24.9 nm was derived for δ of fly ash, representing a constant water layer thickness. Note that this model is based on the computed specific surface area and calibration using fly ash particles as spherical model particles, and is confirmed by the results of other powders. Although this layer thickness is in a similar range like the one derived by Brouwers and Radix [1] being 41.32 nm, there is still a difference of about 40%, which is addressed here.

A most likely explanation is the difference of Blaine surface, used by [1], and computed surface. In the relevant literature most authors agree on linear correlation between Blaine fineness and the surface area calculated from PSD data. [9] found, for instance, a constant factor of 1.3 for the ratio of computed surface area to Blaine. Applying this factor on the data presented would increase the derived δ to 32.4 nm. For the readers interest it is noted, that this constant factor of 1.3, found in [9] is based on the automated surface computation of the deployed laser granulometer [10]. Its computation algorithm is based on a similar principle as the one applied in this study [11, 12]. However, there the geometric mean of a class is considered as mean diameter which results in larger surface areas compared to the arithmetic mean applied here [11]. The difference between both surfaces amounts to about 6% considering a size ratio of $u = 2$ (as being used in standard sieve sets). Furthermore, the underlying model particles are spheres as well. Therefore the surface area difference of 1.3 is based on the assumption of spheres. Considering the true surface of the angular materials, which were actually cements in the example in [9], would turn the deviation even bigger. Therefore, applying

a shape factor in addition to the systematic deviation of Blaine surface and computed surface would result in an increased water layer thickness derived with the presented approach. Depending on the shape factors selected, it is a range of 42 nm to 48 nm when deploying the derived shape factors for blast furnace cements. This correlates with the film thicknesses found in [1] who used Blaine values, and in [7]. High correlation between computed surface area and Blaine fineness was also found in [8], who derived a factor of 0.97. However, the two correlation factors from [8, 9] cannot directly be compared since the latter based the surface area computation on cumulative mass distribution curves derived by sedimentation method. Furthermore, the addressed specific surface area calculation method is based on the assumption of spheres and deploys the arithmetic mean as characteristic diameter. A linear relation of computed specific surface area and measured Blaine surface is manifold confirmed in literature. Varying measurement techniques and different theoretical models, however, make their comparison difficult.

An analysis in this respect for the involved powders resulted indeed in a linear correlation, but with a higher factor. For a number of powders the Blaine value was determined and multiplied with the respective specific density. These values have been plotted versus the computed SSA, now shape-corrected by the addressed model. By means of linear regression a correlation factor of 1.67 was found (i.e. $a = 1.67 a_{Blaine}$), so that:

$$S = 1.67 \cdot a_{Blaine} \cdot \rho_s \tag{7}$$

This increased ratio is explained by the shape correction, which now is included in this consideration. Taken the water layer thickness δ = 41.32 nm from Brouwers and Radix [1] again, which is based on Blaine, and using the derived factor between the surfaces, results in δ = 24.7 nm as well. This should be understood as a correction of the systematic error of Blaine and the sphere assumption of the surface computation models. Hence, both derived water films, δ = 24.7 nm in Brouwers and Radix[1] as well as δ = 24.9 nm with the presented study, are in agreement with each other.

4. CONCLUSION

The present work addresses the spread-flow test or also referred to as mini-slump test. It is demonstrated that, based on simple flow experiments, a shape factor can be derived, which is needed to correct a computed specific surface area, derived from PSD data. This approach is new and shows an interesting alternative to the existing, extensively device-related direct measurement principles. Besides the approach introduced in [6], this is to the author's knowledge the first technique using sound standard measurements for the derivation of a shape factor, which considers form, angularity and surface structure of powder materials. Furthermore, it gives new significance to the spread-flow test. In this regard the hypothesis proposed in [1] is confirmed. According to them the relative slump of a paste becomes a function of the SSA when sufficient water is present for flow.

In this article a water layer thickness of about 25 nm is found for water/powder mixtures on the onset of flowing, i.e. having water contents of $V_w/V_p=\beta_p$. This obtained value corresponds with the figure found in [1]. Different correlations of e.g. Blaine surface and computed SSA have been found in literature, and also proven by own experiments (Eq. (7)). The factor 1.67,

found here, explains the difference in the water layers, but in more general it expresses the difference between true surface and Blaine. Since the Blaine test is a simple and widely-used measurement, the derived correlation can be used to translate Blaine figures into computed figures based on PSDs (or backwards) which appears to result in information of equivalent or better accuracy. Furthermore, also fine particles, not being suitable for Blaine measurement can be expressed as "Blaine values".

The above findings are subject to further analysis and verification in order to find a place in a new concrete mix design concept, which is mainly based on particle size distribution, packing and specific surface area considerations and excess water. Also the hypothesis of constant water layers will be extended to mortars, and presents a new concept for the water demand of mortars and concrete in the framework of mix design.

Acknowledgments

The authors wish to express their sincere thanks to the European Commission (I-Stone Project, Proposal No. 515762-2) and the following sponsors of the research group: Delta Marine Consultants, Bouwdienst Rijkswaterstaat, Rokramix, Betoncentrale Twenthe, Betonmortelcentrale Flevoland, Graniet-Import Benelux, Kijlstra Beton, Struyk Verwo Groep, Hülskens, Insulinde, Dusseldorp Groep, Eerland Recycling, Enci, Provincie Overijssel, Olde Hanter Bouwconstructies, Rijkswaterstaat Directie Zeeland (chronological order of joining)

REFERENCES

[1]. Brouwers H.J.H. & Radix H.J. Self-compacting concrete: theoretical and experimental study. *Cement and Concrete Research* 2005;35:2116-2136, Erratum, ibidem 2007;37:1376.

[2]. Okamura H. & Ozawa K. Mix-design for Self-Compacting Concrete, *Concrete Library, JSCE*, 1995;25:107-120.

[3]. Domone P.L. & HsiWen C. Testing of binders for high performance concrete. *Cement and Concrete Research* 1997;27(8):1141-1147.

[4]. DAfStb - Deutscher Ausschuss für Stahlbeton. Richtlinie „Selbstverdichtender Beton" (SVB-Richtlinie), 'SCC directive' 2001. Berlin: Beuth Verlag GmbH.

[5]. Okamura H. & Ouchi M. (2003), Self-Compacting Concrete, Journal of Advanced Concrete Technology, Japan Concrete Institute, Vol. 1, No. 1, p. 5-15.

[6]. Reschke T. Der Einfluß der Granulometrie der Feinstoffe auf die Gefügeentwicklung und die Festigkeit von Beton. Ph.D. thesis, Bauhaus University Weimar, 2000 (in German).

[7]. Marquardt I. Determination of the composition of self-compacting concretes on the basis of the water requirements of the constituent materials – Presentation of a new mix concept. *Betonwerk + Fertigteiltechnik - BFT* 2002;11:22-30.

[8]. Hunt L.P. & Elspass C.W. Particle-size properties of oilwell cements, *Cement and Concrete Research* 1986;6:805-812.

[9]. Robens E., Benzler B., Büchel G., Reichert H. & Schumacher K. Investigation of characterizing methods for the microstructure of cement, *Cement and Concrete Research* 2002;1:87-90.

[10]. Robens E. (2007), personal contact.

[11]. Hunger M. & Brouwers H.J.H. Flow analysis of water-powder mixtures; Application to specific surface area and shape factor, *Cement and Concrete Composites* 2008, submitted.

[12]. Sympatec GmbH (2001), Software algorithm for the derivation of the PSD-based specific surface area for WINDOX/ HELOS-DOS 4.7 software, Clausthal-Zellerfeld, Germany